Bose-Einstein Condensates in Dilute Atomic Gases

Textbook references:

1. Friedrich, *Theoretical Atomic Physics*, 2nd Ed., Springer, 1998, Section 5.4.
2. Pethick and Smith, *Bose-Einstein Condensation in Dilute Gases*, Cambridge, 2002.
3. C.J. Foot, *Atomic Physics*, Oxford, 2005, Chapter 10 and Appendix F.
4. H.J. Metcalf and P. van der Straten, *Laser Cooling and Trapping*, Springer, 1999, Chapters 12 and 17.

A. Basic Properties of weakly-interacting BECs

Our initial discussion will loosely follow the brief summary of key properties in Foot's book. The starting point is the Bose-Einstein distribution function for N particles with integral spin,

$$f(\varepsilon) = \frac{1}{e^{\beta(\varepsilon-\mu)} - 1}, \quad N = \sum_i f(\varepsilon_i), \tag{1.1}$$

where μ is the *chemical potential* and $\beta = 1/(k_B T)$.

We are interested in the situation where kT is much larger than $\varepsilon_0 - \mu$, where ε_0 is the energy of the ground state of the system. Normally this would lead to the statistical population of many energy levels, but in a BEC, most of the population collapses into the ground state to form a quantum mechanical condensate with a single collective wave function.

In a large sample (on the order of, say, 10^6 atoms), it is a good approximation to neglect μ compared to the excited-state energies. This is valid so long as the number of atoms in the ground state is $N_0 \simeq k_B T/(\varepsilon_0 - \mu) >> 1$, and leads to a much simpler probability distribution for the excited states. This is the same distribution as for photons or other non-interacting bosons,

$$f_{\text{non-int}}(\varepsilon) = \frac{1}{e^{\beta\varepsilon} - 1}, \text{ with } \beta = \frac{1}{k_B T} \tag{1.2}$$

If the number of atoms in the ground state is N_0, we can find the total number of atoms by integrating equation (1.2) over the density of states,

$$N = N_0 + \int_0^\infty f_{\text{non-int}}(\varepsilon)\, AV\sqrt{\varepsilon}\, d\varepsilon \tag{1.3}$$

The ground state number N_0 goes to zero, indicating that there is no significant population in the ground state, at the *critical density*,

$$n_C = \frac{N}{V} = \frac{2.612...}{\lambda_{\text{dB}}^{\,3}}, \text{ where the de Broglie wavelength is } \lambda_{\text{dB}} = \frac{2\pi\hbar}{\sqrt{2\pi m k_B T}}. \tag{1.4}$$

Alternatively, for a given density, the temperature that satisfies Eq. (1.4) is the *critical temperature, T_C*. Below this temperature there will be a finite fraction of the population in the ground state; this is the Bose-Einstein condensate.

Note that the condition (1.4) is nearly equivalent to the obvious criterion that a condensate begins to form when the de Broglie wavelength is comparable to the mean spacing between atoms.

B. Typical Properties of a BEC in a Harmonic Trap

The approximate radius r of a cloud of *thermal* atoms in a harmonic trap can be found by setting

$$\tfrac{1}{2}m\omega^2 r^2 \simeq \tfrac{1}{2}k_B T \tag{1.5}$$

If we ignore the detailed distribution of atoms and write the trap volume as $V \approx \frac{4}{3}\pi r^3$, it follows from Eqs. (1.4) and (1.5) that at the critical temperature, the size of the thermal component is related to the number of atoms and the other parameters by the approximate expression,

$$N^{1/3} \simeq \frac{2.22\,r}{\lambda_{\mathrm{dB}}} = 0.89\frac{k_B T_C}{\hbar\omega}. \tag{1.6}$$

The numerical factor happens to be nearly one, but it will differ depending on the details of the trap and the distribution of atoms. For example, in a harmonically trapped cloud of 10^6 atoms, we find that

$$k_B T_C \simeq N^{1/3}\hbar\omega = 100\hbar\omega. \tag{1.7}$$

This emphasizes the point that at the transition temperature, the atoms occupy many quantum levels of the trap, not just a few, and it is strictly due to quantum statistics, not because of the Boltzmann factor, that the occupation of the ground state becomes very large for $T<T_C$.

For a typical sodium-atom BEC produced in a magnetic trap, we might have ω~100 Hz, so the energy level spacing is $\hbar\omega/k_B = 4.8$ nK. If this trap contains 10^6 atoms, we find from (1.7) that the critical temperature is approximately T_C = 480 nK. The corresponding de Broglie wavelength and density are, from (1.4), λ = 0.53 microns and $n = 1.8\times10^{13}$ cm^{-3}.

B.1. Interactions between atoms in the condensate

At BEC energies, only *s*-wave scattering can occur. Using the relations on p. S-4, we find that the wave function can be written approximately as

$$\psi(r) = A\sin(k(r-a)),\ a \equiv \delta_0/k. \tag{1.8}$$

Here we have reversed the sign of a, relative to the earlier notes, for consistency with Refs. 2-4 at the start of this section of notes. For sufficiently small kr, this becomes just

$$\psi = Ak(r-a)$$

Evaluating the kinetic energy operator $\hbar^2\nabla^2/2m$ by integrating over this wave function from r=0 to ∞, we find an approximate expression for the energy due to interactions between atoms,

$$E_{atom} = \frac{4\pi\hbar^2 a}{m}|A|^2. \tag{1.9}$$

This motivates a widely-used equation that describes the BEC in a mean-field approximation, the *Gross-Pitaevskii equation*,

$$i\hbar\frac{\partial\psi}{\partial t} = \left(-\frac{\hbar^2}{2m}\nabla^2 + V(\mathbf{r}) + g|\psi|^2\right)\psi, \qquad g \equiv \frac{4\pi\hbar^2 a}{m}N, \tag{1.10}$$

where $V(\mathbf{r})$ is the potential due to the trap and any other external perturbations, and the nonlinear interaction $g|\psi|^2$ has the form of (1.9), except that we replace $|A|^2$ by $N|\psi|^2$ to represent the mean interaction energy per atom, in the presence of N other atoms. A much more rigorous derivation is possible, but the present approach helps to explain the physical significance of the nonlinear term in this modified Schrödinger equation. The time-independent version of this equation has as its eigenenergy the chemical potential representing the energy of an individual atom,

$$\left(-\frac{\hbar^2}{2m}\nabla^2 + V(\mathbf{r}) + g|\psi|^2\right)\psi = \mu\psi \tag{1.11}$$

If the scattering length a is negative, an infinite condensate is unstable. Small BECs with negative scattering length were demonstrated very early by Randy Hulet and coworkers, but as the number of atoms grows, they eventually self-destruct in a "Bose-nova". For positive scattering lengths, we can use estimate the size of the condensate using the Gross-Pitaevskii equation:

Assume that the trap is harmonic,

$$V(\mathbf{r}) = \frac{1}{2}m(\omega_x{}^2x^2 + \omega_y{}^2y^2 + \omega_z{}^2z^2). \tag{1.12}$$

If the number of atoms is reasonably large we can neglect the kinetic energy compared to the nonlinear term. In this *Thomas-Fermi* approximation, we need to solve for

$$\left(V(r) + g|\psi|^2\right)\psi = \mu\psi, \tag{1.13}$$

leading immediately to

$$|\psi|^2 = \frac{\mu - V(r)}{g}. \tag{1.14}$$

This gives the density distribution $n|\psi|^2$,

$$n(r) = n_0\left(1 - \frac{x^2}{R_x{}^2} - \frac{y^2}{R_y{}^2} - \frac{z^2}{R_z{}^2}\right), \qquad n_0 \equiv \frac{N\mu}{g}, \tag{1.15}$$

where R_x is defined according to

$$\tfrac{1}{2}m\omega_x{}^2R_x{}^2 = \mu\,, \tag{1.16}$$

and likewise for R_y and R_z. Thus the density profile is an inverted parabola, the mirror image of the trap potential, and it goes to zero at R_i, as shown in the sketch below.

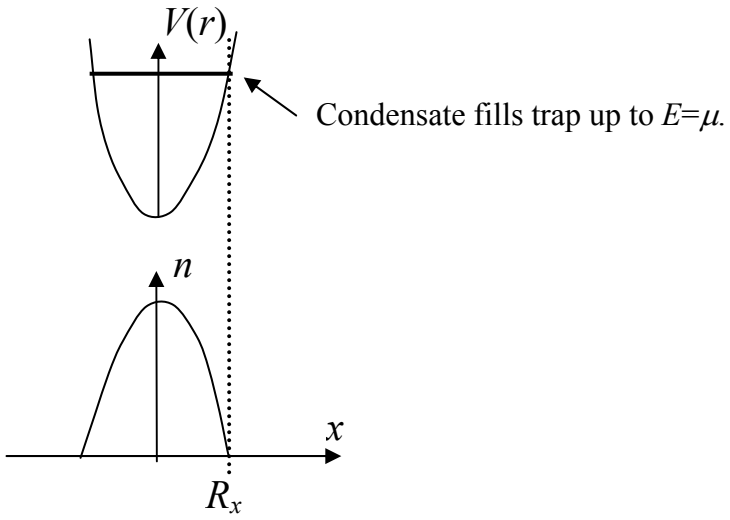

We can solve for the chemical potential using the normalization condition,

$$\iiint |\psi|^2 \, d^3\mathbf{r} = 1 = \frac{\mu}{g}\frac{8\pi}{15} R_x R_y R_z \tag{1.17}$$

Finally, in terms of the radius of the Gaussian ground-state wave function of the harmonic oscillator trap,

$$a_{ho} = \sqrt{\frac{\hbar}{m\bar{\omega}}}, \qquad \bar{\omega} \equiv \left(\omega_x \omega_y \omega_z\right)^{1/3}, \tag{1.18}$$

we can write μ in an easily-evaluated form,

$$\mu = \frac{\hbar\omega}{2}\left(\frac{15Na}{a_{ho}}\right)^{2/5}. \tag{1.19}$$

For the example of a ^{23}Na BEC, the scattering length is a = 2.9 nm. If it consists of 10^6 atoms, and the average trap frequency is $\bar{\omega} = 100$ Hz , we find using Eqs. (1.16), (1.18), and (1.19) that

a_{ho} = 2.1 μm,
μ = 130 nK, expressed in temperature units, and
R = 15 μm (assuming a spherical trap).

So the BEC is much smaller than the thermal cloud, but it is nevertheless significantly larger than the wave function of the ground state of a single atom in the trap in this case by a factor of about seven.

C. Production of BECs

The initial suggestion for a dilute BEC was made by William Stwalley, who proposed that a spin-polarized gas of hydrogen atoms could be made to Bose condense, as the three-body recombination rates are extremely low. This proved to be extremely difficult in practice, and it took a 20-year effort by Daniel Kleppner, Thomas Greytak, and their colleagues to achieve an atomic hydrogen BEC. However, along the way they developed in 1988 the technique that is essential to all current dilute-atom BEC schemes,

C.1. Evaporative Cooling

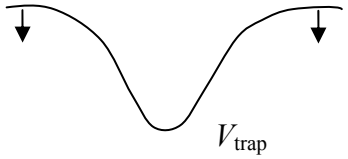

Slowly lower the trap potential to evaporate the hottest atoms.

If elastic collisions are sufficiently rapid, the remaining atoms will re-thermalize and the phase space density will increase. The mechanism is familiar from everyday life---it is the primary means by which a cup of coffee or a bowl of soup cools. The plot on the next page shows actual results for cooling of H atoms, from the initial work at MIT.

While it is easy to write formulas for the energy change in terms of the excess energy in the evaporating atoms, it is less easy to write a complete model for the evaporative cooling process. Some of the details are described by Pethick and Smith, and also by Metcalf and van der Straten. A particularly complete model was recently described by Robert de Carvalho and John Doyle, Phys. Rev. A **70**, 053409 (2004).

Even assuming that the evaporative cooling process works well, there are additional problems in producing a BEC of alkali atoms, including issues involving the trap design:

(a) A MOT cannot be used for $T \lesssim 10\ \mu$K, nor can an ordinary magnetic spherical quadrupole trap, because the losses from nuclear "Majorana" spin flips in the B=0 trap center become excessive.

(b) To get a non-zero minimum in a static B field, a higher-order multipole is needed. This produces a shallow well at the minimum, leading to a spatially extended atom cloud. Thus, the density tends to be low.

Specifically, for an n-pole field the potential depth is related to the radius of the trapped cloud by the scaling rule,

$$U \propto mB_0\left(\frac{r}{R_c}\right)^n, \text{ where } R_c = \text{ radius of coils,} \tag{1.20}$$

so the quadrupole trap (n=2) provides tighter confinement than higher-order traps by a factor of ~10 to 1000.

BEC-6

Evaporative Cooling of Spin-Polarized Atomic Hydrogen

Naoto Masuhara, John M. Doyle, Jon C. Sandberg, Daniel Kleppner, and Thomas J. Greytak
Department of Physics and Center for Materials Science and Engineering, Massachusetts Institute of Technology, Cambridge, Massachusetts 02139

and

Harald F. Hess and Greg P. Kochanski
AT&T Bell Laboratories, Murray Hill, New Jersey 07974
(Received 1 June 1988)

A gas of hydrogen atoms, confined in a static magnetic trap, has been evaporatively cooled to temperatures of a few millikelvin. The initial trap configuration held the gas at 38 mK for as long as 5 h. Evaporative cooling reduced the temperature to 3.0 mK while maintaining the central density at 7.6×10^{12} cm^{-3}. These values were determined by measurement of the rate of electronic spin relaxation and are in agreement with model calculations. Further cooling to 1 mK (inferred from the model) has been achieved. Measurements were made of the efficiency of the evaporative cooling process.

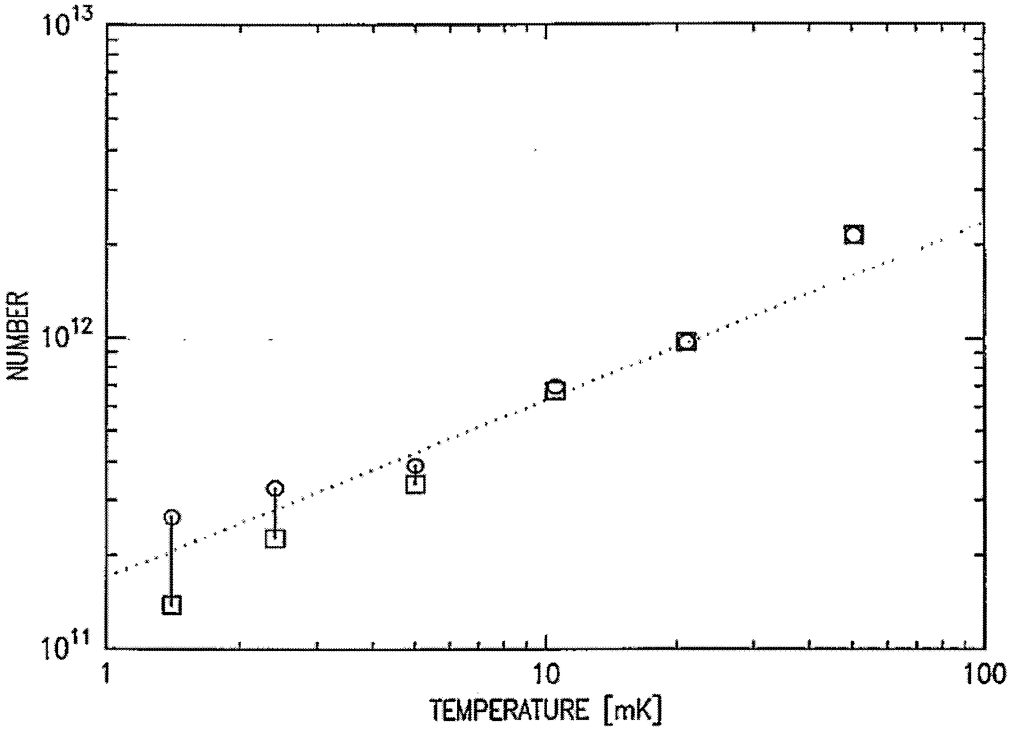

FIG. 3. Number of atoms remaining in the trap after evaporative cooling as a function of temperature. The points represent conditions in the trap just after the fields stop changing. The dotted line corresponds to $N \propto T^{1/1.75}$.

C.2. The "TOP" trap (Petrich *et al.*, Phys. Rev. Lett. **74**, 3352 (1995).

This design, shown on the next page, avoids the problems listed above by a clever and direct solution---continually move the zero of the magnetic field, to keep the atoms away from it! It made possible the first convincing demonstration of a dilute gas BEC, by Anderson, Ensher, Matthews, Wieman, and Cornell, Science **269**, 198 (1995). They used ^{87}Rb, but a second approach using ^{7}Li was demonstrated almost simultaneously, although with a detection method that was initially less convincing (see Bradley, Sackett, Tollett, and Hulet, Phys. Rev. Lett. **75**, 1687 (1995). Later that same year, the group of Wolfgang Ketterle at MIT achieved a BEC in ^{23}Na (Phys. Rev. Lett. **75**, 3969 (1995). These are still the most widely used atoms for BEC work, although several other atoms have now been successfully condensed.

The initial TOP trap experiment combined just about every trick known up to that time for cooling and compressing the atoms in a MOT:

1. Collect atoms in a VCMOT for 300 s, in a background pressure of only ~ 10^{-11} Torr.

2. After about 10^7 atoms accumulate in the dark-spot MOT, they are compressed and cooled to 20 μK by adjusting the B field and the laser frequencies.

3. Next, optical pumping in a small bias magnetic field moves all the atoms to the F=2, m_F=*2* Zeeman sublevel.

4. Now turn off all the lasers and establish a rotating magnetic TOP trap in 1 ms.

5. Ramp up the quadrupole field to increase the elastic collision rate to ~ 3 s^{-1}.

6. Cool evaporatively for 70s (≈trap loss time constant). A ramped rf field controls the evaporation process.

Altogether, the following changes occurred by the time T_C was reached:

4×10^6 atoms 90 μK $n = 2 \times 10^{10}$ cm^{-3}	⟹	2×10^4 atoms 170 nK $n = 2.6 \times 10^{12}$ cm^{-3}

Stable, Tightly Confining Magnetic Trap for Evaporative Cooling of Neutral Atoms

Wolfgang Petrich,* Michael H. Anderson, Jason R. Ensher, and Eric A. Cornell†
Joint Institute for Laboratory Astrophysics, National Institute of Standards and Technology and University of Colorado, and Physics Department, University of Colorado, Boulder, Colorado 80309-0440
(Received 14 November 1994; revised manuscript received 27 February 1995)

We describe a new type of magnetic trap whose time-averaged, orbiting potential (TOP) supplies tight and harmonic confinement of atoms. The TOP trap allows for long storage times even for cold atom samples by suppressing the loss due to nonadiabatic spin flips which limits the storage time in an ordinary magnetic quadrupole trap. In preliminary experiments on evaporative cooling of ^{87}Rb atoms in the TOP trap, we obtain a phase-space density enhancement of up to 3 orders of magnitude and temperatures as low as 200 nK.

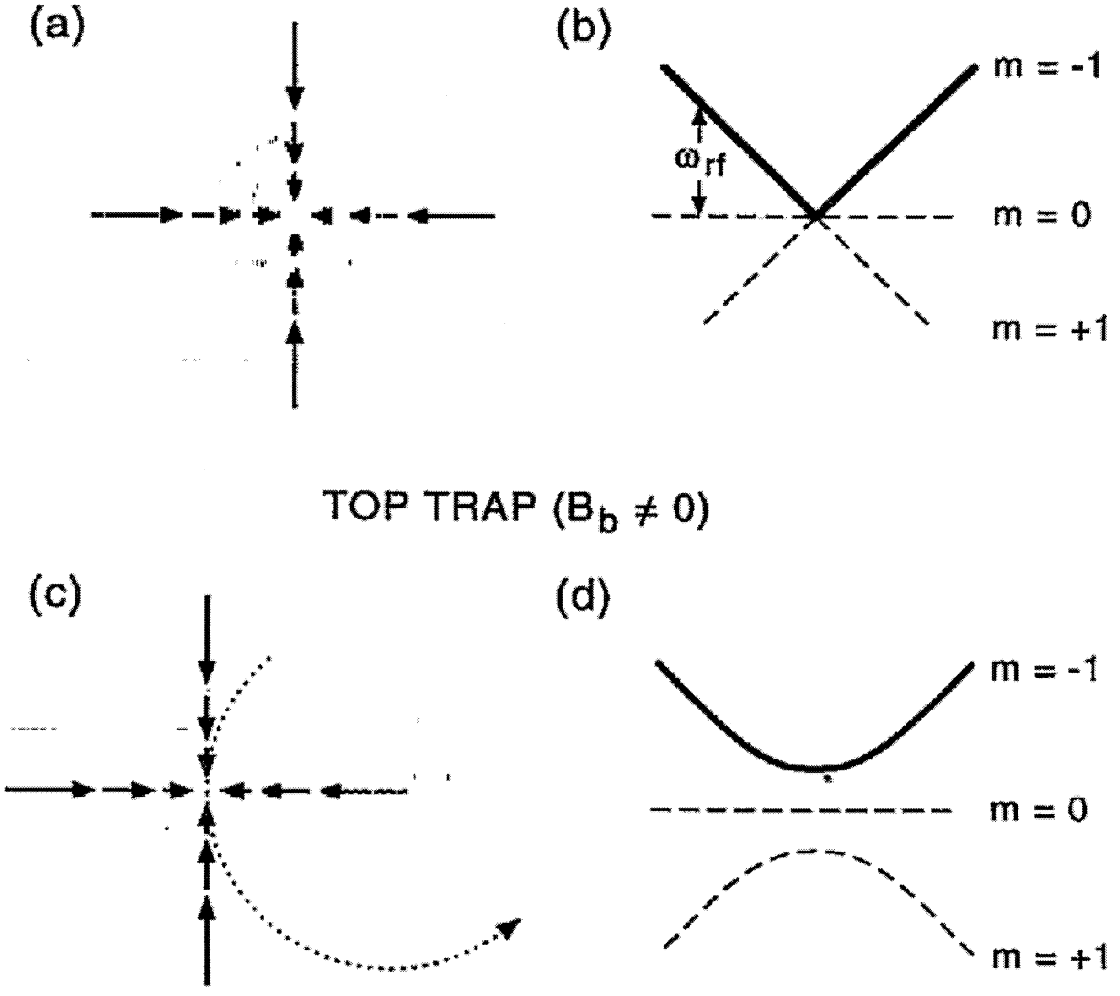

FIG. 1. The magnetic field configuration (a) and the cylindrically symmetric potential (b) of a quadrupole trap. The magnetic field at ω_{rf} for evaporation is shown schematically (b). The instantaneous horizontal field configuration of the TOP trap (c) is displayed together with the time-averaged, orbiting potential (d) of this new type of trap. In both the quadrupole potential and the TOP potential, an atom like ^{87}Rb is considered, which is trapped in a state with the total angular momentum quantum number $F = 1$ and the magnetic quantum number $m = -1$.

C.2. The Ioffe-Pritchard trap

By adding a bias field along the *z* axis to a quadrupole trap, the bottom of the trapping potential can be rounded off, which (a) eliminates the zero-field point, and (b) makes the well harmonic near the bottom. A good description, with illustrations, can be found in Foot's book. The illustration below is from Dieckmann, Spreeuw, Weidemüller, and Walraven, Phys. Rev. A **58**, 3891 (1998). Miniaturized "atom chip" versions have also been developed. These traps are useful not only for forming BECs, but also for storing them afterwards.

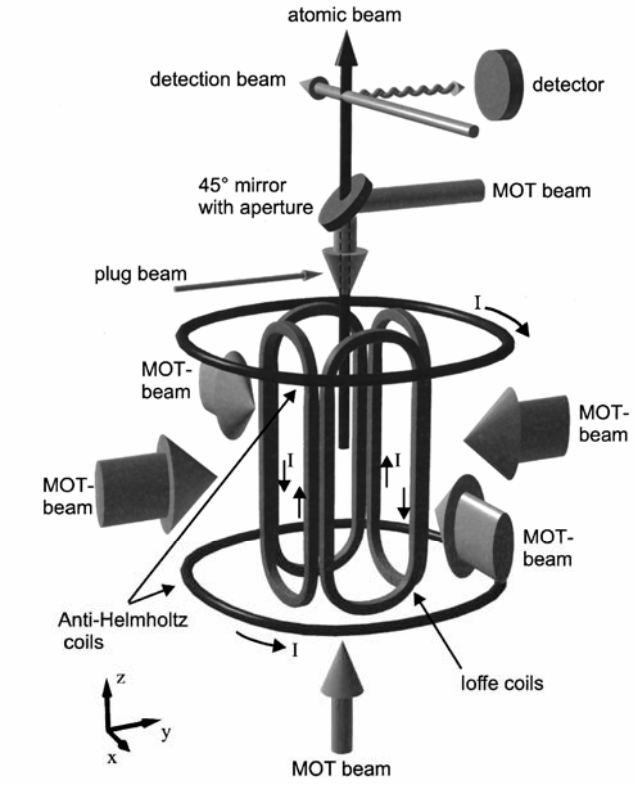

FIG. 1. Experimental setup: The rubidium vapor cell from which the atomic beam is extracted is located inside the four racetrack-shaped magnetic field coils. These so-called Ioffe coils produce a two-dimensional quadrupolar magnetic field and are used in the 2D-MOT and $2D^+$-MOT configurations. The anti-Helmholtz coils are used for the three-dimensional quadrupolar field necessary for the LVIS configuration. The vertical MOT beams used for the $2D^+$-MOT and the LVIS are absent in the 2D-MOT case. After passing through an aperture in a 45° mirror into an ultrahigh vacuum chamber, the atomic beam is detected by means of fluorescence.

C.2. Evaporation in an optical trap

The production of a BEC in a QUEST-type optical trap is very appealing in principle, but so far only a few successful realizations. The first was by Barrett, Sauer, and Chapman, Phys. Rev. Lett. **87**, 010404 (2001). A single-beam version has recently been developed by the group of M Weitz at Tübingen.

Vortex Formation in a Stirred Bose-Einstein Condensate

K. W. Madison, F. Chevy, W. Wohlleben,* and J. Dalibard
Laboratoire Kastler Brossel,† Département de Physique de l'Ecole Normale Supérieure, 24 rue Lhomond, 75005 Paris, France

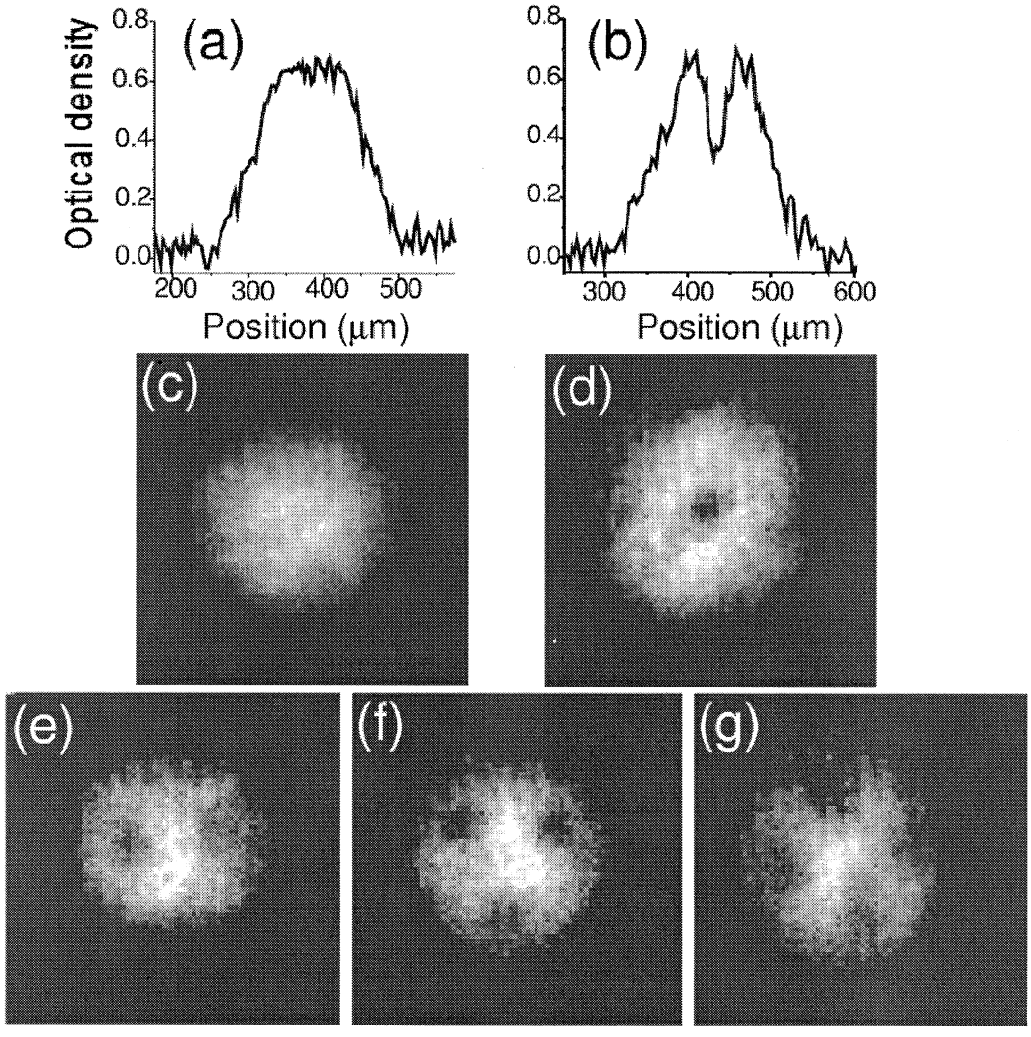

FIG. 1. Transverse absorption images of a Bose-Einstein condensate stirred with a laser beam (after a 27 ms time of flight). For all five images, the condensate number is $N_0 = (1.4 \pm 0.5)\ 10^5$ and the temperature is below 80 nK. The rotation frequency $\Omega/(2\pi)$ is, respectively, (c) 145 Hz, (d) 152 Hz, (e) 169 Hz, (f) 163 Hz, (g) 168 Hz. In (a) and (b) we plot the variation of the optical thickness of the cloud along the horizontal transverse axis for the images (c) (0 vortex) and (d) (1 vortex).

Atom Lasers

A. The rf Output Coupler

A simple but legitimate atom laser can be formed by coupling out a portion of a condensate in a way that retains its coherence. One method is to use rf pulses to transfer the population to an untrapped state:

^{23}Na ground state in magnetic trap

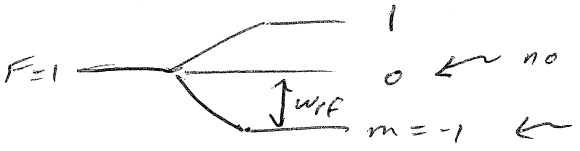

← no response to $\vec{B}$ field (in 1st order)

← trapped

This was accomplished by Ketterle's group (Mewes et al., PRL 78, 582 (1997). A much-improved version has been demonstrated by Bloch, Hänsch, and Esslinger, PRL 82, 3008 (1999): "Atom Laser with a cw Output Coupler."

In its simplest form, the output coupler provides an adjustable mix of the trapped state (call it $|1\rangle$) and the untrapped state ($|2\rangle$), according to

$$\cos\left(\omega_R \frac{\tau}{2}\right) |1\rangle + \sin\left(\omega_R \frac{\tau}{2}\right) |2\rangle$$

The untrapped state departs because of a) gravity, and b) the repulsive effective force between atoms, typically a smaller effect.

A more careful treatment takes into account that a) the B field is quadratic in (average) magnitude as a function of position, and b) the condensate is displaced below the B field minimum by $d = \frac{g}{\omega_\perp^2}$ (= 7.67 μm for Bloch et al, with $\frac{\omega_\perp}{2\pi} = 180$ Hz).

The figure on p. BEC-13 depicts the full situation. For a given value of B, the group of atoms that can be decoupled is specified by the intersection of an ellipsoid and the condensate volume.

In the experiment, B_{rf} is ramped from $0 \to 2.6$ mG over a 0.1 ms period, then left on for 15 msec. The frequency is ramped from 1.752 $\to$ 1.750 MHz to accomodate the shrinking condensate cloud ($R \propto N^{3/5}$ in the Thomas-Fermi approximation.) The figure on p. BEC-14 shows the resulting beam of 2×10^5 coherent atoms, after falling for another 3.5 ms.

$\Delta v_z \sim 3 \frac{mm}{s}$ (Fourier limit is $0.3 \frac{mm}{s}$)

$\Delta v_y = \Delta v_x \sim 5 \frac{mm}{s}$ (from chemical potential; diffraction limit would be smaller)

$$\text{Brightness} \equiv \frac{\text{flux}}{\text{source area}} \frac{1}{\Delta v_x \Delta v_y \Delta v_z}$$

$$= 2 \times 10^{24} \text{ atoms } s^2 \text{ } m^{-5}$$

(ideally 4×10^{28} if Fourier/diffraction limited.)

By contrast, the best beam sources provide about

2.9×10^{18} atoms s^2 m^{-5},

and of course they are far less coherent.

B. The stimulated Raman output coupler

See pp. BEC-15 $\to$ BEC-17 for an account. Two lasers are used to impart momentum $\vec{p} = \pm(\vec{k}_1 - \vec{k}_2)$, $p = 2\hbar k \sin\frac{\theta}{2}$, and to simultaneously change the state of m. The transverse momentum spread is only $\approx 0.004\ \hbar k$, because most of the energy release from the chemical potential is channeled in the forward direction.

Atom Laser with a cw Output Coupler

Immanuel Bloch, Theodor W. Hänsch, and Tilman Esslinger

Sektion Physik, Ludwig-Maximilians-Universität, Schellingstrasse 4/III, D-80799 Munich, Germany and Max-Planck-Institut für Quantenoptik, D-85748 Garching, Germany

(Received 3 December 1998)

We demonstrate a continuous output coupler for magnetically trapped atoms. Over a period of up to 100 ms, a collimated and monoenergetic beam of atoms is continuously extracted from a Bose-Einstein condensate. The intensity and kinetic energy of the output beam of this atom laser are controlled by a weak rf field that induces spin flips between trapped and untrapped states. Furthermore, the output coupler is used to perform a spectroscopic measurement of the condensate, which reveals the spatial distribution of the magnetically trapped condensate and allows manipulation of the condensate on a micrometer scale. [S0031-9007(99)08914-0]

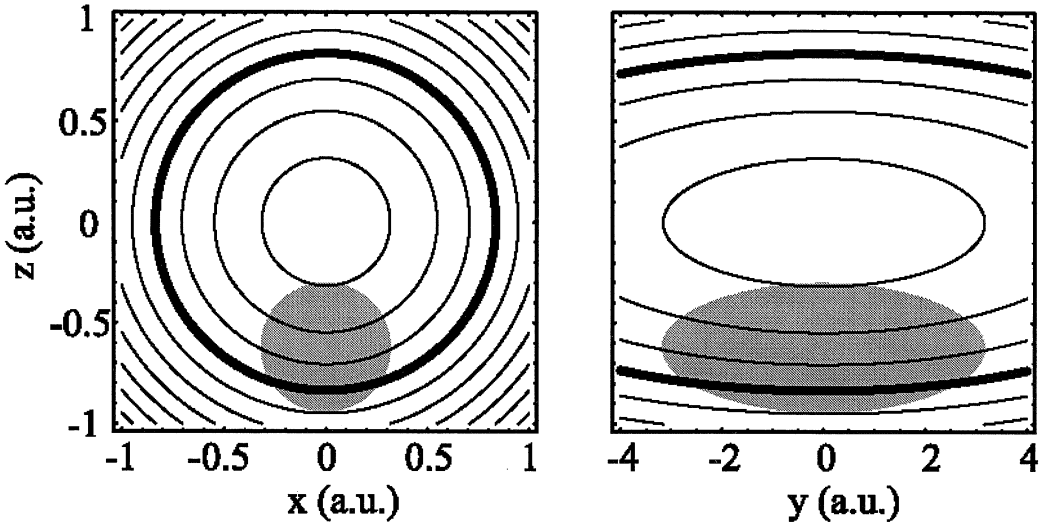

FIG. 2. Continuous output coupling from a Bose-Einstein condensate. The contour lines represent the absolute value of the magnetic trapping field. The thick line indicates the region where the rf field transfers atoms from the magnetically trapped state into an untrapped state. Because of gravity, the condensate is trapped 7.67 μm below the minimum in the magnetic field. In the untrapped state the atoms experience a directed force caused by gravity and the mean field of the condensate. This results in a collimated output beam.

Atom Laser with a cw Output Coupler

Immanuel Bloch, Theodor W. Hänsch, and Tilman Esslinger

Sektion Physik, Ludwig-Maximilians-Universität, Schellingstrasse 4/III, D-80799 Munich, Germany and Max-Planck-Institut für Quantenoptik, D-85748 Garching, Germany

(Received 3 December 1998)

We demonstrate a continuous output coupler for magnetically trapped atoms. Over a period of up to 100 ms, a collimated and monoenergetic beam of atoms is continuously extracted from a Bose-Einstein condensate. The intensity and kinetic energy of the output beam of this atom laser are controlled by a weak rf field that induces spin flips between trapped and untrapped states. Furthermore, the output coupler is used to perform a spectroscopic measurement of the condensate, which reveals the spatial distribution of the magnetically trapped condensate and allows manipulation of the condensate on a micrometer scale. [S0031-9007(99)08914-0]

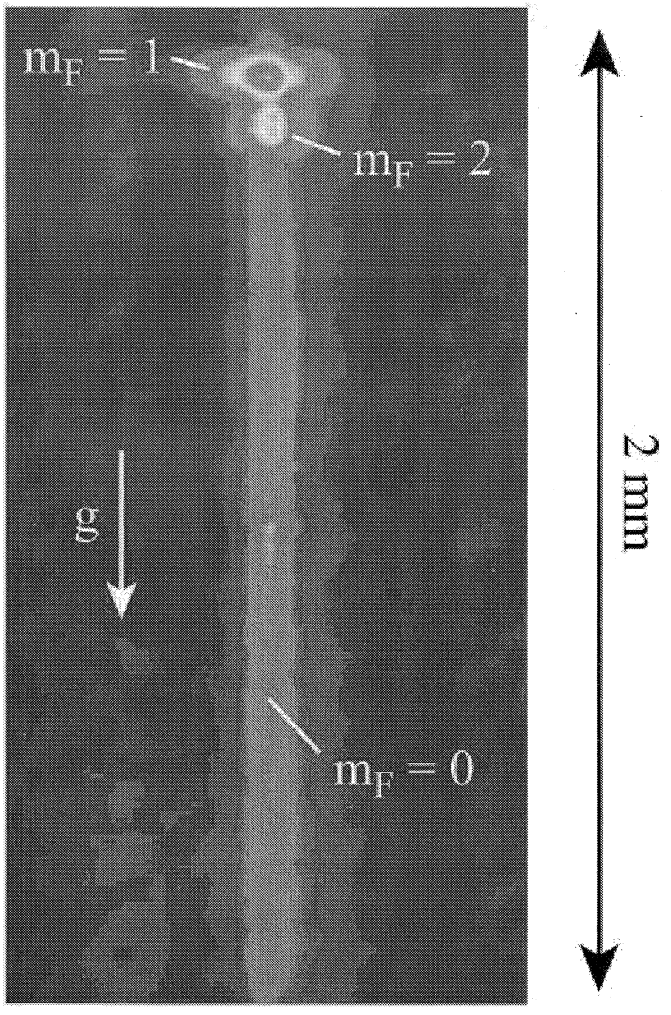

FIG. 1(color). Atom laser output: A collimated atomic beam is derived from a Bose-Einstein condensate over a 15 ms period of continuous output coupling. A fraction of condensed atoms has remained in the magnetically trapped $|F = 2, m_F = 2\rangle$ and $|F = 2, m_F = 1\rangle$ state. The magnetic trap has its weakly confining axis in the horizontal direction.

BEC-15

From: "A Well Collimated Quasi-Continuous Atom Laser"

E.W. Hagley, L. Deng, M. Kozuma, J. Wen, K. Helmerson, S.L. Rolston, and W. D. Phillips, Science 283, 1706 (1999)

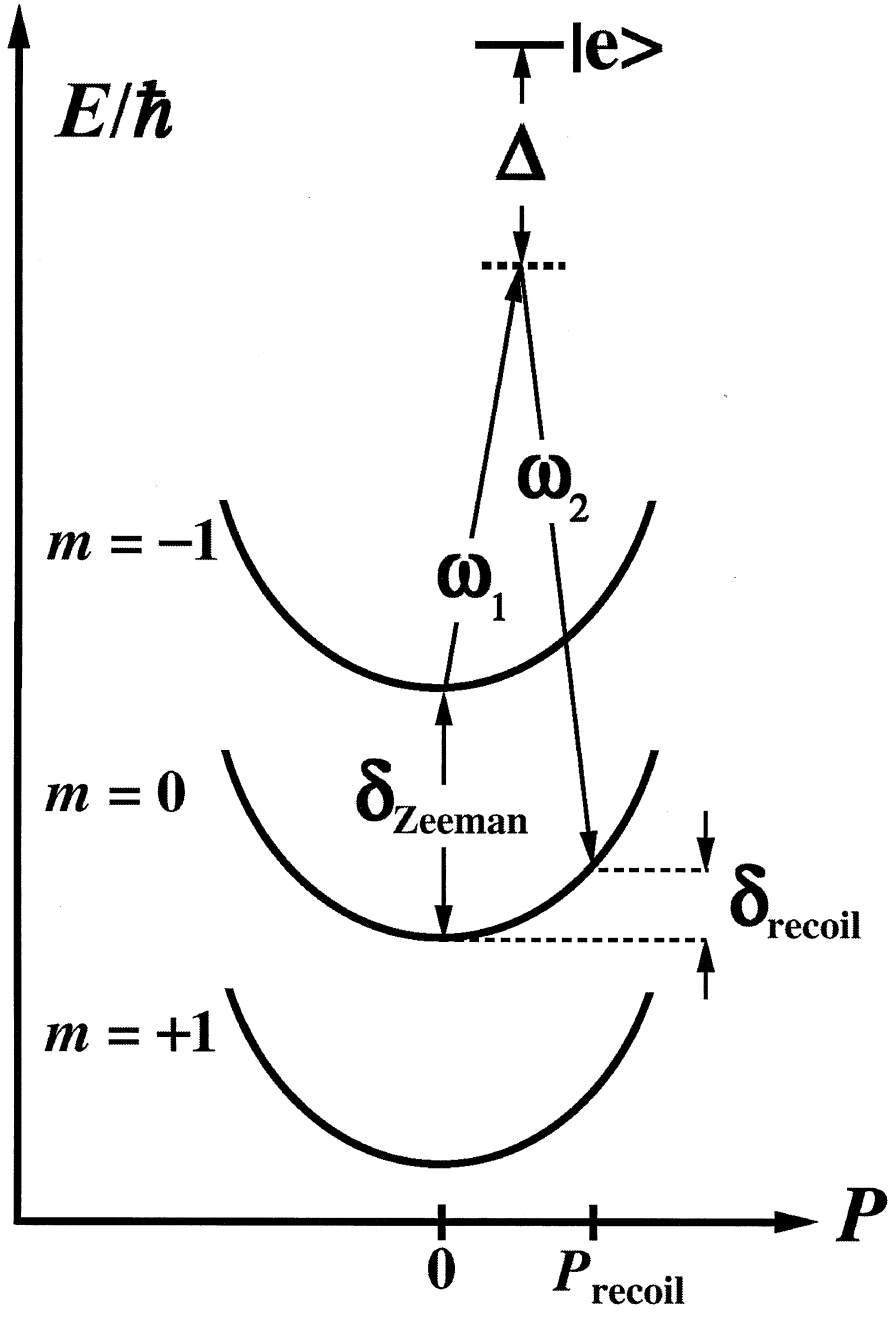

Fig. 1 Principle of the Raman output coupler. Energy conservation requires a relative detuning, $\delta = \omega_2 - \omega_1$, between the Raman lasers. Total energy as a function of atomic momentum is plotted, where the parabolas correspond to kinetic energy $P^2/2M$.

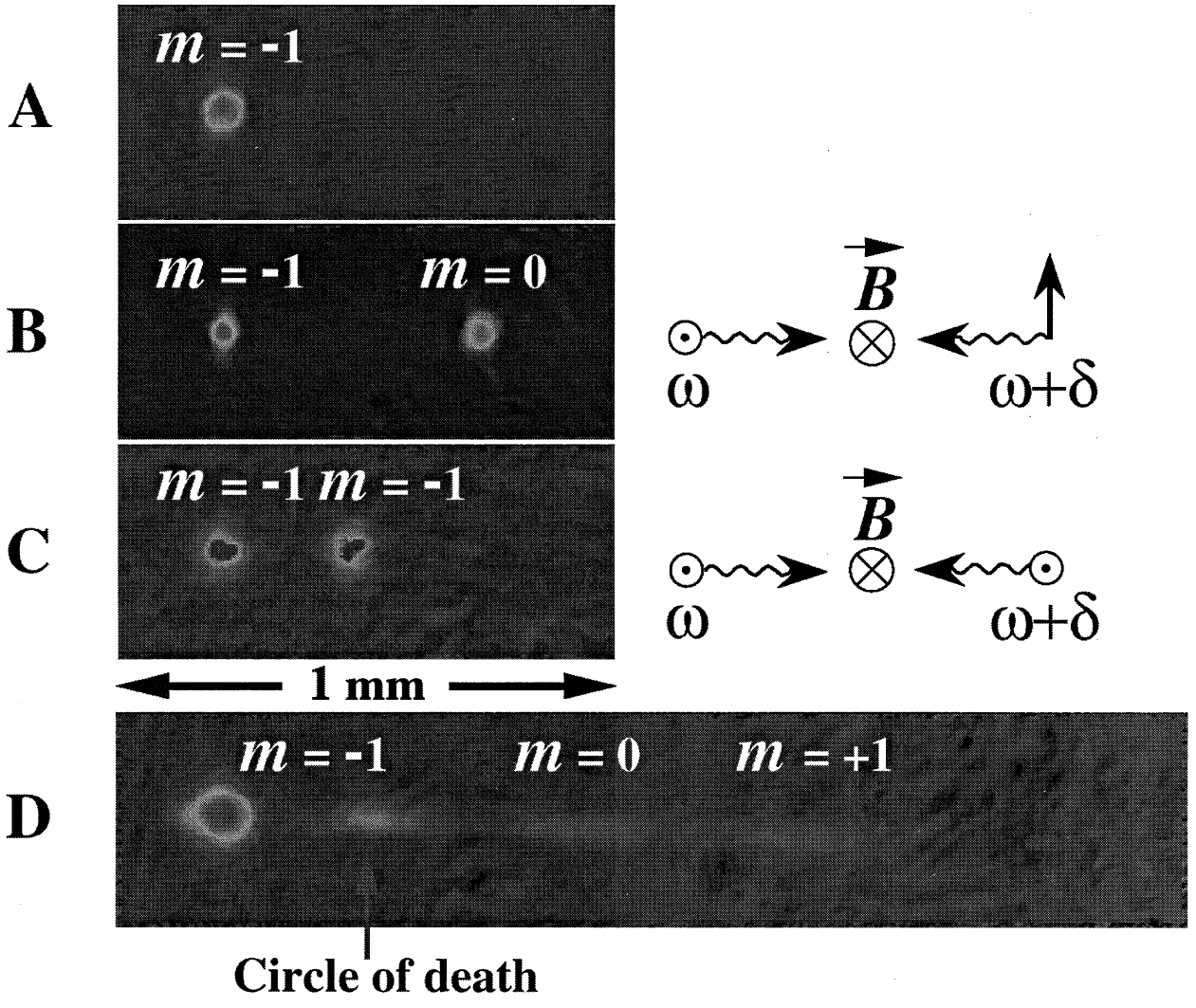

Fig. 2 (A) Condensate before the application of a Raman pulse. (B) $\Delta m = +1$ transition (19) from a 6 μs pulse with $\delta / 2\pi = 6.4\,\mathrm{MHz}$. This detuning is chosen to be slightly larger than the 6.27 MHz resonance frequency to suppress four-photon coupling to the $m = +1$, $4\hbar k\hat{z}$ state (25). (C) $\Delta m = 0$ transition (26) after a 14 μs Raman pulse with equal laser intensities of $25\,\mathrm{mW/cm^2}$. The relative detuning was $\delta/2\pi = -98\,\mathrm{kHz}$ and the polarizations of both lasers were aligned with $\hat{x}$. The diagrams to the right of (B) and (C) show the polarization of the lasers with respect to the local magnetic field. We verified that no transitions occurred when incorrect polarizations were used. (D) The rotating magnetic field zero (circle of death) results in Majorana transitions of an output-coupled condensate fraction in the $m = 0$ state. The arrow denotes the physical location of the rotating bias field zero. This is a graphic depiction of Majorana transitions.

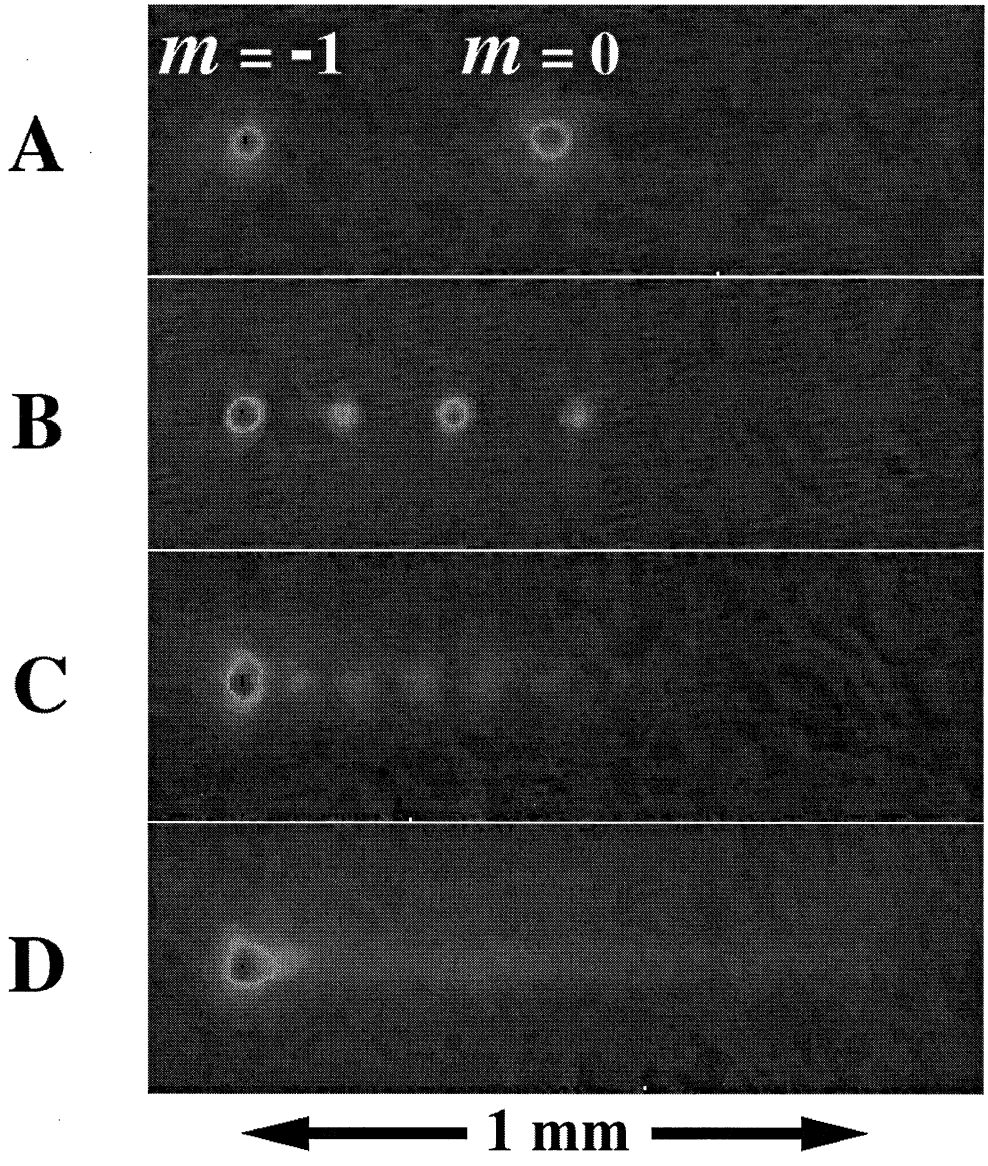

Fig. 4. In Fig. 4A-C, one, three and six 6 μs Raman pulses were applied to the condensate, respectively. (D) Firing 1μs Raman pulses at the full repetition rate of ~20 kHz imposed by the frequency of the rotating bias field (140 pulses in 7 ms) produces a quasi-continuous atomic beam.

Nonlinear Atom Optics

A fascinating property of coherent atom optics was pointed out by Trippenbach, Band, and Julienne, Opt. Express 3, 530 (1998). A single-component BEC is described by the intrinsically nonlinear Gross-Pitaevskii eqn,

$$i\hbar \frac{\partial \Psi}{\partial t} = \left(-\frac{\hbar^2}{2M}\nabla^2 + V + U_0 |\Psi|^2 \right) \Psi$$

V: trap; $U_0 = \frac{4\pi a_0 \hbar^2}{m}$ (atom-atom interaction); N

Thus, four-wave mixing is possible with no external medium, provided

1) $\sum \vec{k} = 0$

2) energy is conserved

and 3) particle number is conserved.

Experimental realization: Deng et al., 1999 (see following three pages).

Because of condition 3), matter-wave 4WM can always be viewed as degenerate 4WM in an appropriate moving frame.

Perhaps more useful is the view that two atom waves set up a standing wave, from which a third wave is Bragg diffracted.

In any case, theoretical modeling agrees very closely with experiment. Also, scaling laws work well —

if $\Psi = \sum_{i=1}^{4} \Psi_i$, initially $\frac{\partial \Psi_4}{\partial t} \propto \Psi_1 \Psi_2^* \Psi_3$

In the Thomas-Fermi limit,

$$\frac{N_4}{N} \propto N_1^{\circ} N_2^{\circ} N_3^{\circ} N^{-9/5},$$ verified closely!

BEC-19

From: "Nonlinear Atom Optics: Multi-wave mixing with matter waves"

L. Deng, E.W. Hagley, J. Wen, M. Trippenbach, Y. Band, P.S. Julienne, J.E. Simsarian, K. Helmerson , S.L. Rolston, and W.D. Phillips, Nature **398**, 218 (1999).

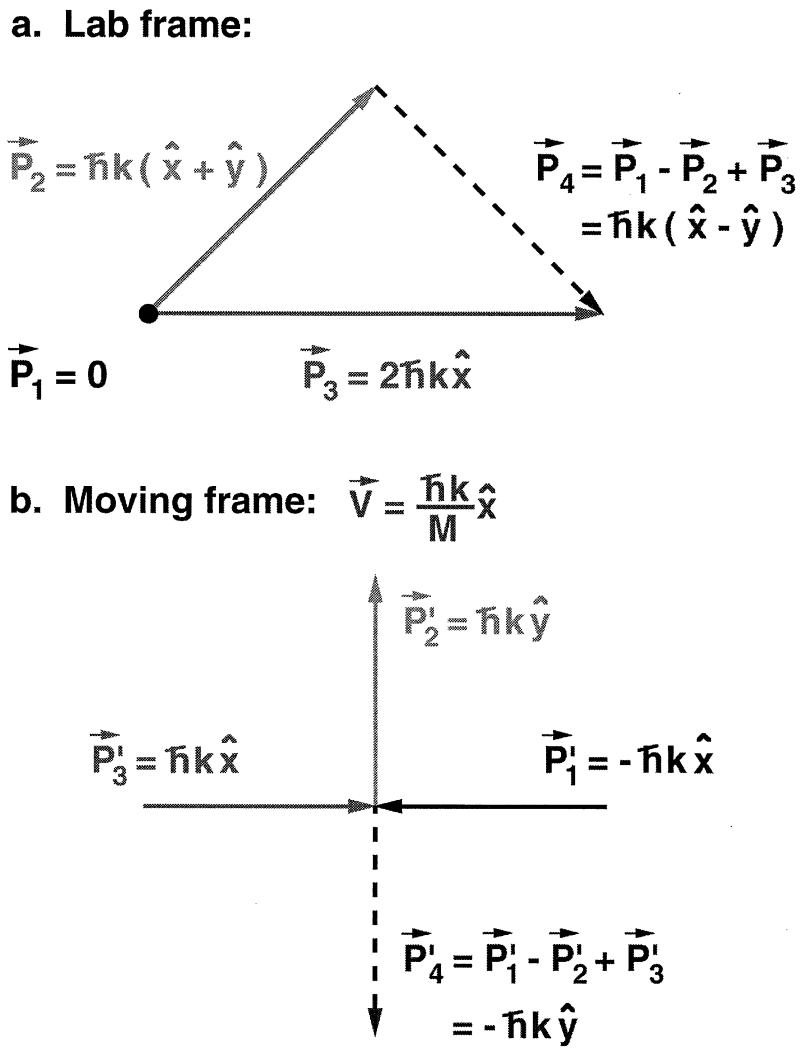

Figure 1a. Momentum conservation, $\vec{P}_4 = \vec{P}_1 - \vec{P}_2 + \vec{P}_3$, (equivalent to phase-matching in optical 4WM) in the laboratory frame. Energy conservation requires $\vec{P}_4^{\,2} = \vec{P}_1^{\,2} - \vec{P}_2^{\,2} + \vec{P}_3^{\,2}$.

Figure 1b. It is always possible to view matter 4WM in a frame moving with velocity $\vec{v}$ such that the three input momenta have the same magnitude, and two are counter-propagating. Then, in our case two atoms in momentum states $\vec{P}_1' = -\hbar k\hat{\mathbf{x}}$ and $\vec{P}_3' = \hbar k\hat{\mathbf{x}}$ are bosonically stimulated by wavepacket $\vec{P}_2' = \hbar k\hat{\mathbf{y}}$ to scatter into momentum states $\vec{P}_2'$ and $\vec{P}_4' = -\vec{P}_2' = -\hbar k\hat{\mathbf{y}}$. Notice that the energy and momentum conditions are satisfied independent of the direction of $\vec{P}_2'$. The 4WM wavepacket is a consequence of energy, momentum and particle number conservation when atoms are stimulated into the momentum state $\vec{P}_2'$. Thus, 4WM can be viewed as the annihilation of momentum states $\vec{P}_1'$ and $\vec{P}_3'$, and the creation of momentum states $\vec{P}_2'$ and $\vec{P}_4'$ (the minus signs in the energy and momentum conditions are attached to the state that gains atoms). It is this bosonic stimulation of scattering that mimics the stimulated emission of photons from an optical nonlinear medium. Alternatively, by choosing a frame of reference in which $\vec{P}_1'' = -\vec{P}_2''$ (or $\vec{P}_2'' = -\vec{P}_3''$), 4WM can also be viewed as matter-wave Bragg diffraction of $\vec{P}_3''$ ($\vec{P}_1''$) from the grating produced by the interference of two others.

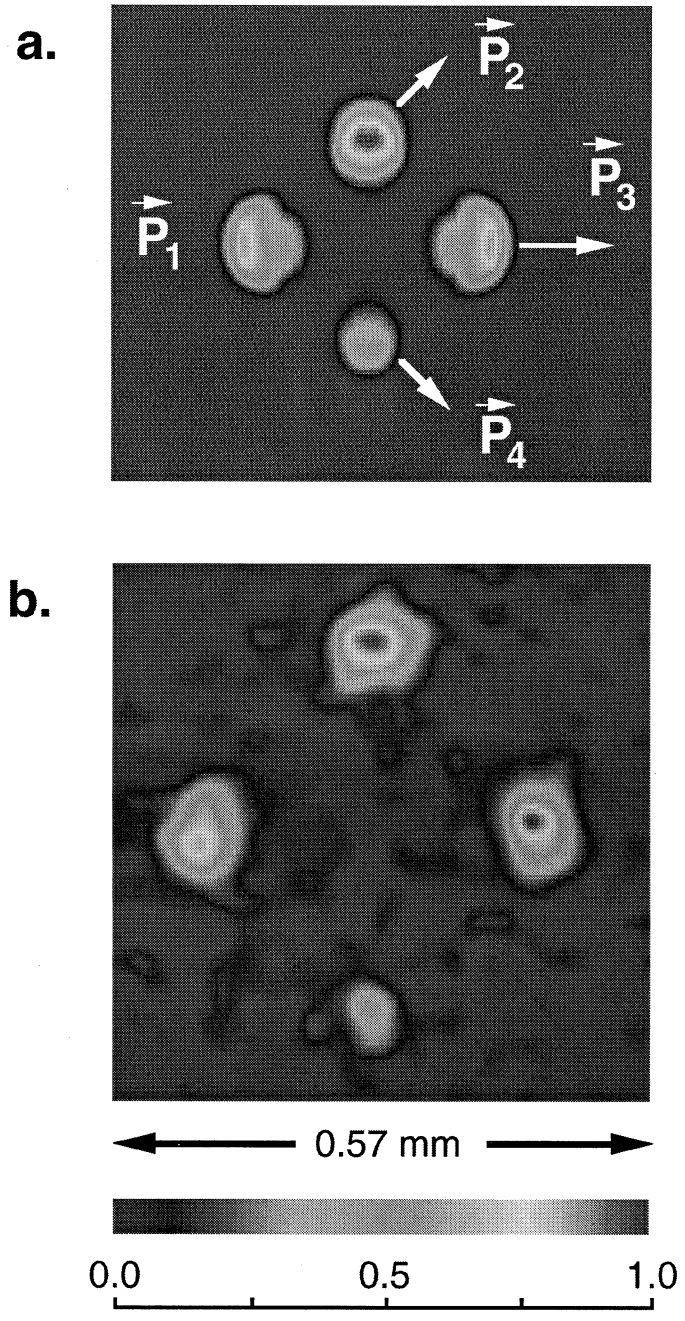

Figure 2a. Calculated 2-D atomic distribution after 1.8 ms showing the 4WM. The calculations were performed only until the wavepackets completely separated due to constraints on the simulation grid-size. The momenta are those of Figure 1a. The field of view is 0.23 mm by 0.26 mm. Notice that atoms are removed primarily from the back-end of the wavepackets because these regions overlap for the longest time.

Figure 2b. A false-color image of the experimental atomic distribution showing the fourth (small) wavepacket generated by the 4WM process. The four wavepackets form a square measuring 0.26 mm by 0.26 mm, corresponding to the distance of 0.25 mm calculated using the experimental time of flight of 6.1 ms and the wavepacket momenta. We have verified that if we make initial wavepackets such that energy and momentum conservation cannot be simultaneously satisfied, no 4WM signal is observed. For instance, if we change the sign of the frequency difference between the two laser beams that comprise the second Bragg pulse, we will create a component with momentum $\vec{P}_3 = -2\hbar k\hat{\mathbf{x}}$ instead of $\vec{P}_3 = 2\hbar k\hat{\mathbf{x}}$. In this case there is no 4WM signal.

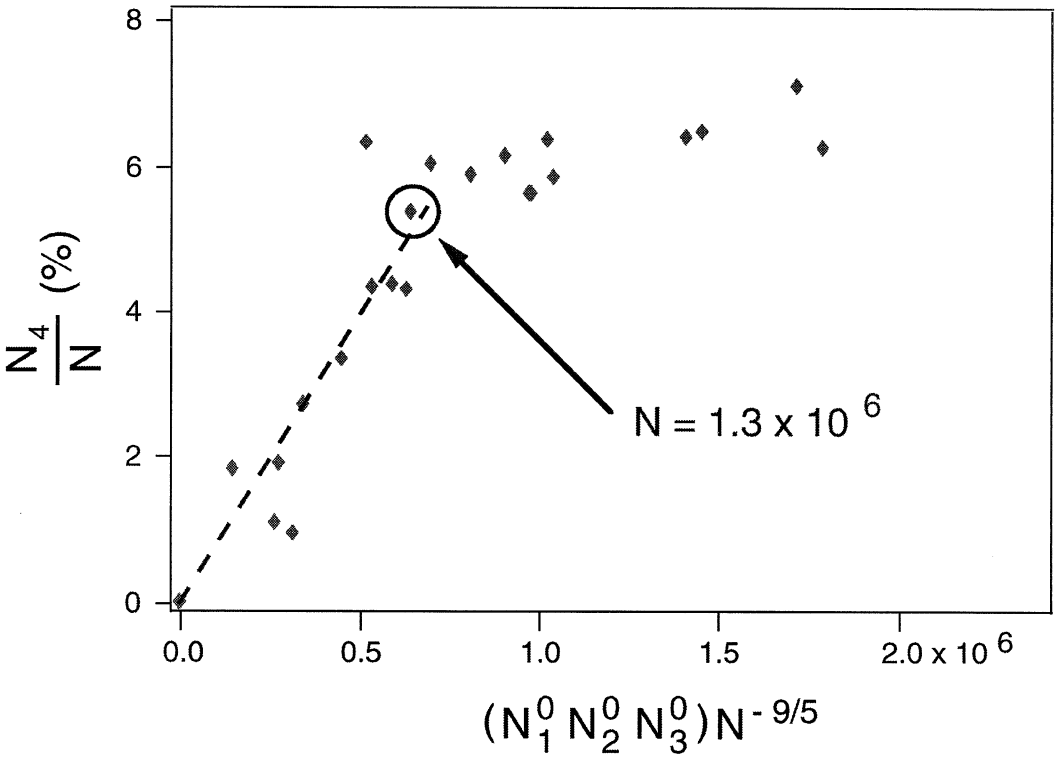

Figure 3. Efficiency $\frac{N_4}{N}$ as a function of $(N_1^0 N_2^0 N_3^0) N^{-9/5}$. The initial linear dependence is a signature of 4WM with matter waves. The dashed line is a fit to the first 12 points to guide the eye.

Superconductor ↔ Mott insulator transition

Observed by Bloch and coworkers, Nature 415, 39 (2002).

Place a BEC in an optical lattice:

are atoms localized??

For small V, Ψ is a delocalized Bloch state, and BEC phase and superfluidity are preserved. If V(r) is suddenly turned off and atoms freely expand, a high-contrast interference pattern is seen (see next page).

If V(r) is large enough that atomic interactions > tunneling interaction, a quantum phase transition occurs

Bloch state ⟶ Fock state, pure # state for each site (insulator).

Remarkably, if V(r) is ~~slowly~~ restored, the BEC coherence very rapidly redevelops.

Previously used as theoretical model for liquid He, but this is a much cleaner realization. Theoretical treatment centers on the Bose-Hubbard model,

$$H = -J \sum_{\text{pairs}} \hat{a}_i^\dagger \hat{a}_j + \sum \epsilon_i \hat{n}_i + \frac{1}{2} U \sum \hat{n}_i (\hat{n}_i - 1)$$

$\hat{n}_i = \hat{a}_i^\dagger \hat{a}_i$ = number operator at site i.

ϵ_i = external lattice potential " " ".

$U = \frac{4\pi\hbar^2 a}{m} \int |w(\vec{r})|^4 d^3\vec{r}$ ← Wannier fcn at site i.

BEC-23

Quantum phase transition from a superfluid to a Mott insulator in a gas of ultracold atoms

Markus Greiner*, Olaf Mandel*, Tilman Esslinger†, Theodor W. Hänsch* & Immanuel Bloch*

* *Sektion Physik, Ludwig-Maximilians-Universität, Schellingstrasse 4/III, D-80799 Munich, Germany, and Max-Planck-Institut für Quantenoptik, D-85748 Garching, Germany*

† *Quantenelektronik, ETH Zürich, 8093 Zurich, Switzerland*

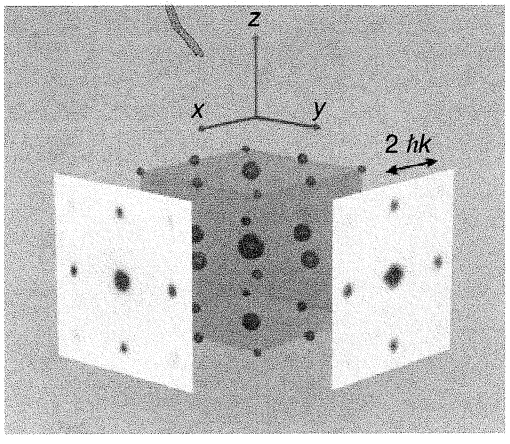

Figure 1 Schematic three-dimensional interference pattern with measured absorption images taken along two orthogonal directions. The absorption images were obtained after ballistic expansion from a lattice with a potential depth of $V_0 = 10E_r$ and a time of flight of 15 ms.

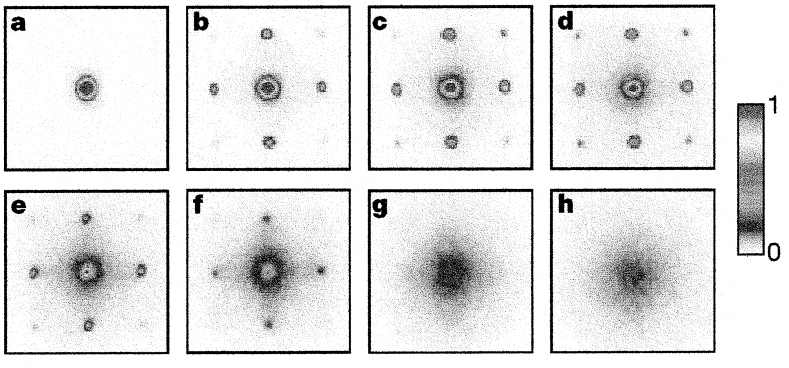

Figure 2 Absorption images of multiple matter wave interference patterns. These were obtained after suddenly releasing the atoms from an optical lattice potential with different potential depths V_0 after a time of flight of 15 ms. Values of V_0 were: **a**, 0 E_r; **b**, 3 E_r; **c**, 7 E_r; **d**, 10 E_r; **e**, 13 E_r; **f**, 14 E_r; **g**, 16 E_r; and **h**, 20 E_r.

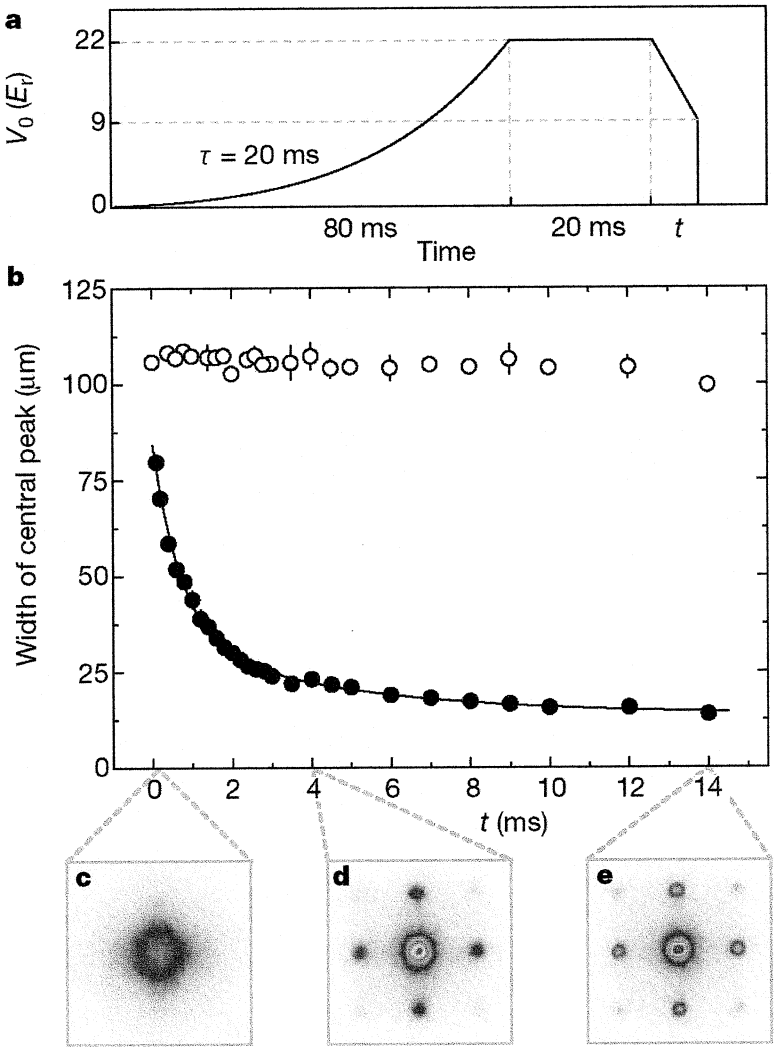

Figure 3 Restoring coherence. **a**, Experimental sequence used to measure the restoration of coherence after bringing the system into the Mott insulator phase at $V_0 = 22E_r$ and lowering the potential afterwards to $V_0 = 9E_r$, where the system is superfluid again. The atoms are first held at the maximum potential depth V_0 for 20 ms, and then the lattice potential is decreased to a potential depth of 9 E_r in a time t after which the interference pattern of the atoms is measured by suddenly releasing them from the trapping potential. **b**, Width of the central interference peak for different ramp-down times t, based on a lorentzian fit. In case of a Mott insulator state (filled circles) coherence is rapidly restored already after 4 ms. The solid line is a fit using a double exponential decay ($\tau_1 = 0.94(7)$ ms, $\tau_2 = 10(5)$ ms). For a phase incoherent state (open circles) using the same experimental sequence, no interference pattern reappears again, even for ramp-down times t of up to 400 ms. We find that phase incoherent states are formed by applying a magnetic field gradient over a time of 10 ms during the ramp-up period, when the system is still superfluid. This leads to a dephasing of the condensate wavefunction due to the nonlinear interactions in the system. **c–e**, Absorption images of the interference patterns coming from a Mott insulator phase after ramp-down times t of 0.1 ms (**c**), 4 ms (**d**), and 14 ms (**e**).

Production of Molecular BECs using Feshbach Resonances

The term "Feshbach resonance" is used in a rather specialized sense in ultracold physics. It refers specifically to hyperfine-related structure, usually in the presence of Zeeman tuning in an external magnetic field. A good example of Zeeman-tuning a resonance to zero energy is seen in calculations by F.H. Mies, E. Tiesinga, and P.S. Julienne, Phys. Rev. A **61**, 022721 (2000):

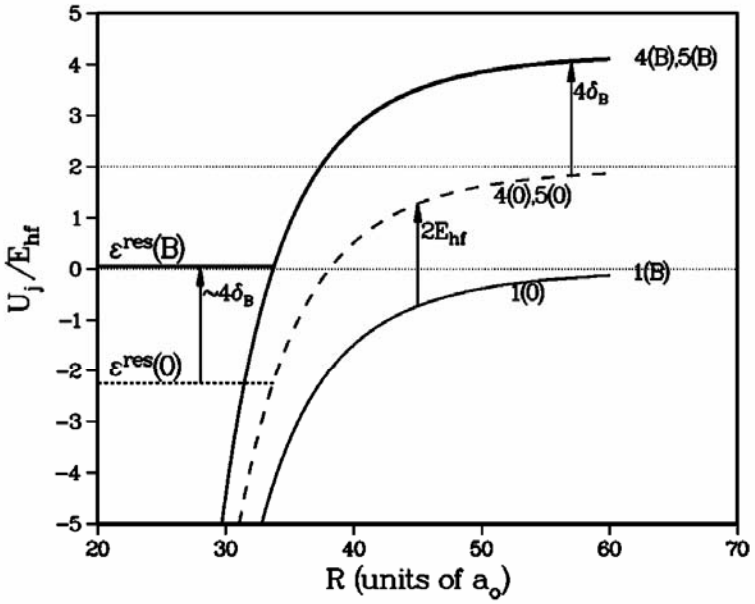

FIG. 2. Three of the five adiabatic potentials U_j of the $m=2$ s-wave scattering process are shown as functions of internuclear separation. The dashed curves correspond to $B=0$ adiabatic potentials and are labeled $j(0)$, while the solid curves correspond to $B=91$ mT adiabatic potentials and are labeled $j(B)$, where in general j is 1, 2, 3, 4, or 5 in order of increasing energy. However, for clarity the $j=2$ and 3 curves are omitted. For both B values the zero of energy is set at the $R\rightarrow\infty$ asymptote of the $j=1$ adiabatic potential. For the range of internuclear separation shown the adiabatic potentials 1(0) and $1(B)$ are identical. As is explained in the text, the two Feshbach resonances are due to weak coupling to bound states in the $j=4$ and 5 adiabatic potentials. The vibrational levels $\epsilon_n^{res}(0)$ and $\epsilon_n^{res}(B)$ show the relevant bound state for $B=0$ and $B=91$ mT, respectively. On the energy scale of the figure the $j=4$ and 5 Feshbach resonances are indistinguishable. The arrow labeled $2E_{hf}$ indicates the $B=0$ splitting between level 1(0) and levels 4(0) or 5(0). The arrows labeled $4\delta_B$ show that the energy shift of the asymptotic energies of state 5 from $B=0$ to $B=91$ mT is approximately equal to the energy shift of the bound states.

By tuning the position of the molecular resonance through degeneracy with the energy of a pair of unbound atoms, molecules can be created. The following illustration is from S. Dürr, T. Volz, A. Marte, and G. Rempe, Phys. Rev. Lett. **92**, 020406 (2004):

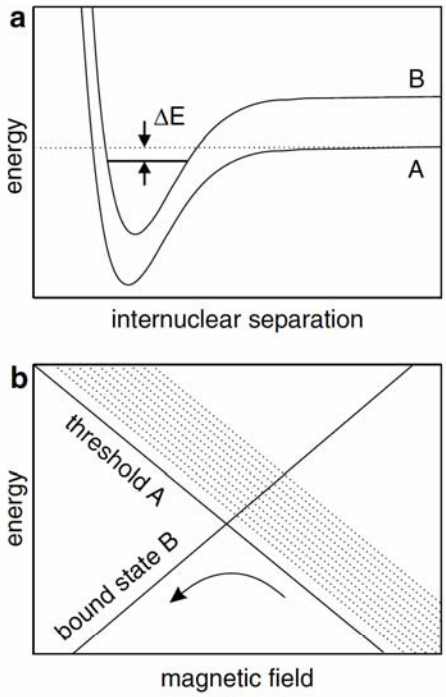

FIG. 1. Theory of Feshbach resonances. (a) Molecular potentials involved in a Feshbach resonance. Potential A corresponds to the entrance channel and potential B to a closed channel of the scattering process. Potential B supports a bound state (solid straight line), to which the incoming wave function can couple. The energy of an incoming pair of cold atoms is very close to the dissociation threshold (dotted line). For $\Delta E \rightarrow 0$, the population of the bound state is resonantly enhanced. (b) Creation of cold molecules using a Feshbach resonance. The energy of the dissociation threshold and the molecular bound state are shown as a function of magnetic field (solid lines). An atomic BEC can be converted into molecules using an adiabatic rapid passage. The experiment uses a negative ramp speed ($dB/dt < 0$), as indicated by the arrow. For positive ramp speed, the existence of noncondensate states of atom pairs (dotted lines) would prevent the buildup of a large molecular fraction.

Several groups have used this method, with some variations, to achieve a Bose-Einstein condensate of bosonic molecules, formed from fermionic atoms. This includes the groups of Deborah Jin ($^{40}K_2$), Wolfgang Ketterle ($^{6}Li_2$), Rudi Grimm ($^{6}Li_2$), and Randy Hulet ($^{6}Li_2$).

Another fascinating feature of this method is that the scattering length can be tuned arbitrarily by varying the position of the resonance. This allows the study of the crossover from a "molecular" BEC (at positive scattering length) to a BCS-type state with Cooper pairing of distant atoms, as well as the strongly-coupled region in between. One such result is the article *Experimental Study of the BEC-BCS Crossover Region in Lithium 6*, by T. Bourdel, *et al.*, Phys. Rev. Lett. **93**, 050401 (2004):

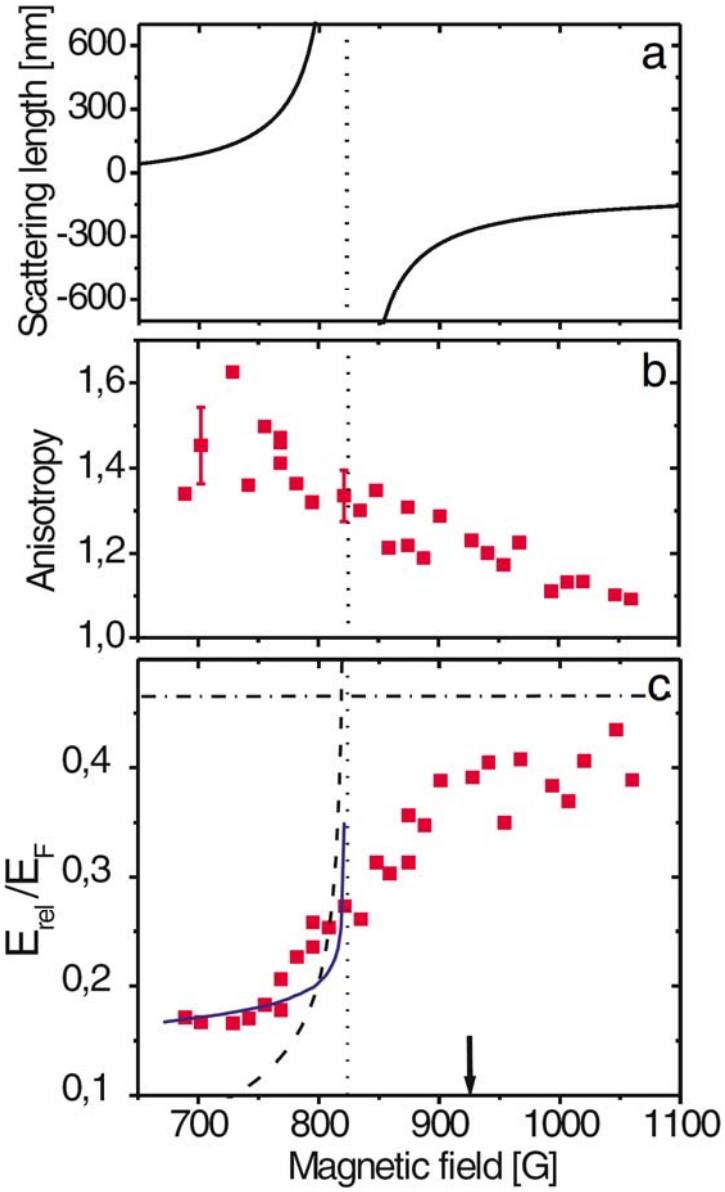

FIG. 3 (color online). (a) scattering length between the $|1/2, 1/2\rangle$ and $|1/2, -1/2\rangle$ ^{6}Li states. The Feshbach resonance peak is located at 822 G (dotted line). (b): anisotropy of the cloud, (c) release energy across the BEC-BCS crossover region. In (c), the dot-dashed line corresponds to a $T = 0$ ideal Fermi gas. The dashed curve is the release energy from a pure condensate in the Thomas-Fermi limit. The solid curve corresponds to a finite temperature mean field model described in the text with $T = 0.6\,T_C^0$. Arrow: $k_F|a| = 3$.